TRPM2 mediates ischemic kidney injury and oxidant stress through RAC1

Guofeng Gao,[1] Weiwei Wang,[1] Raghu K. Tadagavadi,[1] Nicole E. Briley,[1] Michael I. Love,[1] Barbara A. Miller,[2] and W. Brian Reeves[1]

[1]Division of Nephrology, Department of Medicine, and [2]Division of Hematology and Oncology, Department of Pediatrics, Penn State Milton S. Hershey Medical Center and College of Medicine, Hershey, Pennsylvania, USA.

Ischemia is a leading cause of acute kidney injury. Kidney ischemia is associated with loss of cellular ion homeostasis; however, the pathways that underlie ion homeostasis dysfunction are poorly understood. Here, we evaluated the nonselective cation channel transient receptor potential melastatin 2 (TRPM2) in a murine model of kidney ischemia/reperfusion (I/R) injury. TRPM2-deficient mice were resistant to ischemic injury, as reflected by improved kidney function, reduced histologic damage, suppression of proapoptotic pathways, and reduced inflammation. Moreover, pharmacologic TRPM2 inhibition was also protective against I/R injury. TRPM2 was localized mainly in kidney proximal tubule epithelial cells, and studies in chimeric mice indicated that the effects of TRPM2 are due to expression in parenchymal cells rather than hematopoietic cells. TRPM2-deficient mice had less oxidative stress and lower levels of NADPH oxidase activity after ischemia. While RAC1 is a component of the NADPH oxidase complex, its relation to TRPM2 and kidney ischemic injury is unknown. Following kidney ischemia, TRPM2 promoted RAC1 activation, with active RAC1 physically interacting with TRPM2 and increasing TRPM2 expression at the cell membrane. Finally, inhibition of RAC1 reduced oxidant stress and ischemic injury in vivo. These results demonstrate that TRPM2-dependent RAC1 activation increases oxidant stress and suggest that therapeutic approaches targeting TRPM2 and/or RAC1 may be effective in reducing ischemic kidney injury.

Introduction

Acute kidney injury (AKI) is a frequent clinical event associated with serious complications and an unacceptably high mortality rate. Ischemia is a major cause of AKI in both native and transplanted kidneys (1, 2). One of the early hallmarks of kidney ischemia is loss of intracellular potassium and increases in intracellular sodium, chloride, and calcium (3–5). The pathways responsible for this loss of ion homeostasis are incompletely understood but involve a reduction in sodium-potassium ATPase activity as well as activation of poorly characterized leak pathways (6). Although blockers of ion channels have shown some efficacy in certain models of kidney injury (6–11), the molecular identity of the specific ion channels that mediate AKI in vivo remains unknown.

TRPM2 was the second member of the transient receptor potential melastatin subfamily to be cloned and is expressed in many cell types including hematopoietic, endothelial, and kidney cells (12–14). TRPM2 has been shown to play an important role in cell proliferation and oxidant-induced cell death in a variety of in vitro settings (15–17). While several TRP channels are expressed in the kidney and are involved in disease states such as polycystic kidney disease and focal segmental glomerulosclerosis (18, 19), the role of TRPM2 in kidney physiology or pathophysiology is unknown.

TRPM2 is permeable to calcium, potassium, and sodium and is activated by oxidant stress, ADP-ribose (ADPR), TNF-α, and intracellular calcium (20–23). Each of these stimuli is increased during kidney ischemia (24, 25). These observations prompted us to hypothesize that TRPM2 channels are activated during kidney ischemia and participate in organ damage. In this study, we found that mice with a targeted deletion of TRPM2 are protected from ischemic AKI. Likewise, pharmacologic inhibition of TRPM2 reduced kidney ischemic injury. Oxidant stress is a mediator of kidney ischemia/reperfusion (I/R) injury (26). We found that deletion of TRPM2 was associated with a reduction in oxidant stress, NADPH oxidase activity, and apoptosis in the kidney. Active RAC1 translocates to the plasma membrane with NADPH oxidase and increases the production of ROS (27). However, the role of RAC1 in AKI and the possible interactions between TRPM2 and RAC1 in AKI have never been examined. Our results indicate that RAC1 is activated in a TRPM2-dependent manner and leads to oxidant production and kidney injury after ischemia. Finally, our results show that the effects of TRPM2 on ischemic AKI are mediated by TRPM2 expressed on parenchymal cells rather than hematopoietic cells. Thus, these studies have identified important novel roles for TRPM2 and RAC1 in ischemic kidney injury and indicate that these pathways may be targeted to prevent AKI.

Results

TRPM2 is expressed in kidney proximal tubules. Immunofluorescence demonstrated expression of TRPM2 in tubular epithelial cells throughout the cortex and outer medulla (Figure 1). Double labeling with *Lotus tetragonolobus* lectin (LTL), which binds to the brush border of the proximal tubule (28), indicated that TRPM2 was expressed almost exclusively in the proximal tubule, although not all proximal tubules had high levels of TRPM2. We detected no signal in glomeruli (not shown) or in peritubular endothelial or interstitial cells. Staining within the proximal tubule cells (PTCs)

Conflict of interest: The authors have declared that no conflict of interest exists.
Submitted: March 10, 2014; **Accepted:** September 4, 2014.
Reference information: *J Clin Invest.* 2014;124(11):4989–5001. doi:10.1172/JCI76042.

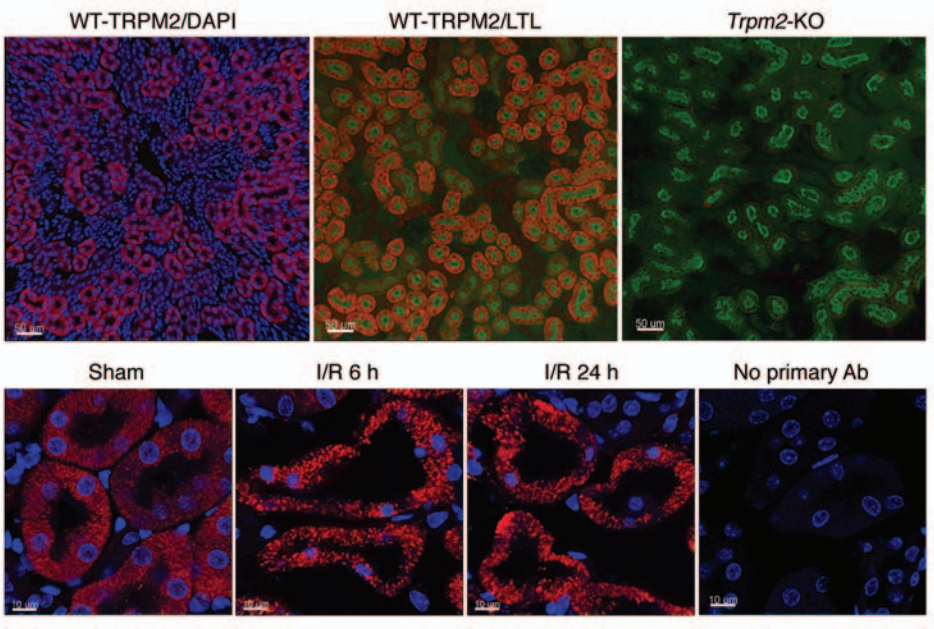

Figure 1. Localization of TRPM2 in the kidney. Top row: Kidney sections were labeled with a TRPM2 Ab (red), DAPI (blue), and LTL (green), a marker of proximal tubules. Bottom row: Confocal images of TRPM2 (red) and DAPI-stained sections from kidneys harvested after sham surgery or 6 and 24 hours after I/R. Sections from TRPM2-deficient mice (top right) or sections stained without incubation with the TRPM2 Ab (bottom right) served as negative controls. Scale bars: 50 μm (top panels), 10 μm (bottom panels).

was diffuse, without definite plasma membrane localization. After I/R, the distribution of TRPM2 became more punctate, but total kidney levels of TRPM2 protein and mRNA did not change significantly (Supplemental Figure 1, D and E; supplemental material available online with this article; doi:10.1172/JCI76042DS1).

Trpm2-KO mice are resistant to ischemic kidney injury. To explore the role of TRPM2 in I/R-induced AKI, *Trpm2*-KO mice and WT control mice were subjected to 28 minutes of bilateral kidney ischemia followed by reperfusion (29, 30). As shown in Figure 2A and Supplemental Figure 1A, WT mice developed kidney failure, as reflected by increases in blood urea nitrogen (BUN) and creatinine, while *Trpm2*-KO mice had less kidney dysfunction. We found that kidney function was not affected by sham surgery and that baseline BUN and creatinine values did not differ between genotypes (Supplemental Figure 1B). *Trpm2*-KO mice also had less severe histologic kidney damage after I/R than did WT mice, as shown by less cast formation, preservation of brush border membranes, less sloughing of epithelial cells (Figure 2, C and E), and less induction of lipocalin 2 (NGAL, Figure 2E), a marker of kidney injury (31). Ischemic kidney injury results in inflammation and infiltration of the kidney by neutrophils (32). We observed that I/R dramatically increased neutrophil infiltration in WT kidneys as determined by flow cytometry (Figure 2, D and E) and immunohistochemistry (Supplemental Figure 2). In contrast, we observed significantly fewer neutrophils in *Trpm2*-KO kidneys. Heterozygous deletion of TRPM2 did not afford any protection from ischemic AKI (Supplemental Figure 1C), indicating that a partial presence of TRPM2 is sufficient to promote injury and that the C-terminal truncation in the *Trpm2*-KO mouse did not act as a dominant-negative (DN) inhibitor of the WT TRPM2 channel.

Since TRPM2 is permeable to calcium and potassium, we measured the tissue content of calcium and potassium in kidneys harvested 6 hours after surgery. Ischemia produced a significant decrease in potassium and an increase in tissue calcium in both WT and KO mice (Table 1). Although *Trpm2*-KO mice had smaller changes in tissue electrolyte content than did WT mice, these differences were not statistically significant.

Pharmacologic inhibition of TRPM2 prevents ischemic kidney injury. Treatment of WT mice with 2-aminoethoxydiphenyl borate (2-APB), an inhibitor of TRPM2 (33), prior to I/R resulted in a dramatic reduction in kidney dysfunction (Figure 2B). Since 2-APB may affect other calcium channels (34), we also treated the *Trpm2*-KO mice with 2-APB. 2-APB produced no additional improvement in kidney function in the absence of TRPM2. Administration of 2-APB either 1 or 6 hours after reperfusion also reduced ischemic injury, whereas protection was lost when the administration was delayed until 12 hours after reperfusion (Supplemental Figure 3). Collectively, these results demonstrate that deletion or inhibition of TRPM2 in mice results in better preservation of kidney function and tissue morphology and reduced neutrophil infiltration after kidney ischemia.

We also examined the role of TRPM2 in pigment- and drug-induced AKI (Supplemental Figure 4). We found that TRPM2 deficiency was associated with less severe glycerol-induced AKI, while the severity of cisplatin-induced AKI was not altered by the absence of TRPM2.

Table 1. Elemental composition of kidney cortex

	Potassium (mg/g wet weight)	Calcium (mg/g wet weight)
Sham (n = 8)	2.78 ± 0.1	0.015 ± 0.01
WT I/R (n = 8)	2.25 ± 0.3, P = 0.01 vs. sham	0.057 ± 0.02, P = 0.01 vs. sham
Trpm2-KO I/R (n = 8)	2.48 ± 0.1, P = 0.001 vs. sham	0.037 ± 0.02, P = 0.02 vs. sham

Kidneys were harvested 6 hours after 28 minutes of ischemia or sham surgery. The content of potassium and calcium in the kidney cortex was determined by atomic absorption spectroscopy. The electrolyte content of sham kidneys from WT and KO mice was indistinguishable, and the results were combined in the table (n = 4 each for sham WT and sham KO mice).

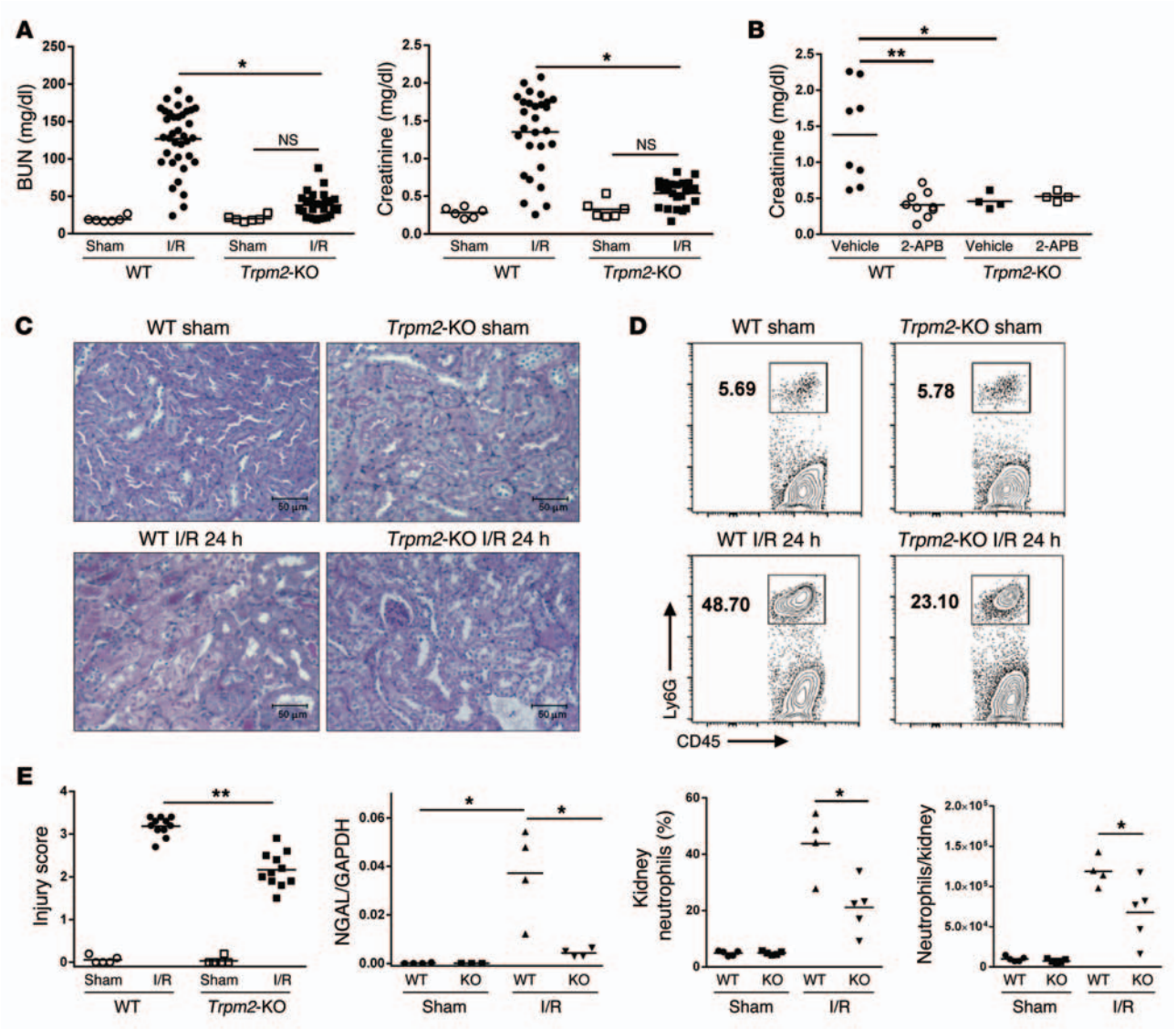

Figure 2. Deletion or pharmacologic inhibition of TRPM2 reduces ischemic AKI. (**A**) *Trpm2*-KO and WT mice were subjected to 28 minutes of bilateral kidney ischemia or sham surgery. Blood collected 24 hours after surgery was analyzed for BUN and serum creatinine as measures of kidney function. (**B**) Serum creatinine in WT and *Trpm2*-KO mice were pretreated with 2-APB or vehicle and then subjected to bilateral kidney ischemia. (**C**) PAS-stained kidney tissue sections from *Trpm2*-KO and WT mice subjected to kidney ischemia or sham surgery. Scale bars: 50 μm. (**D**) FACS analysis of neutrophils in kidneys from *Trpm2*-KO and WT mice subjected to kidney ischemia or sham surgery. Numbers denote the percentage of CD45 cells that were also Ly6G$^+$. (**E**) Quantification of tubular injury, NGAL expression, and neutrophil infiltration. $^*P < 0.05$; $^{**}P < 0.01$.

TRPM2 in parenchymal cells mediates ischemic injury. In addition to PTCs (Figure 1), TRPM2 is expressed in other cell types including hematopoietic cells (13). TRPM2 has been reported to influence the response of neutrophils, monocytes, and dendritic cells to inflammation (13, 35, 36). Since inflammation is a mediator of I/R injury, it was possible that TRPM2 expressed on hematopoietic cells might account for the resistance of *Trpm2*-KO mice to kidney ischemia. To define the location of the TRPM2 that mediates kidney ischemic injury, bone marrow chimeric mice were created, in which TRPM2 was deleted in either hematopoietic cells or parenchymal cells. As shown in Figure 3A, chimeric mice with parenchymal expression of TRPM2, i.e., WT→WT or KO→WT chimeric mice, developed severe ischemic kidney injury, whereas mice that lacked TRPM2 expression in parenchymal cells, i.e., WT→KO and KO→KO chimeras, suffered relatively little kidney dysfunction. Histologic tissue injury (Figure 3B) and the extent of kidney neutrophil infiltration (Supplemental Figure 5) followed a similar pattern, with less injury and neutrophil influx in the chimeric mice, which lacked TRPM2 in nonhematopoietic parenchymal cells. In contrast, the presence or absence of TRPM2 in bone marrow–derived cells had no impact on ischemic kidney injury. These results suggest that kidney parenchymal TRPM2 is critical for I/R-induced kidney injury. To examine this issue further, we determined the susceptibility of proximal tubule epithelial cells isolated from WT and *Trpm2*-KO mice to hypoxic stress in vitro. We assessed cell viability using the MTT assay (Figure 3C) and observed that *Trpm2*-KO and WT PTCs exhibited similar proliferation and viability under normal culture conditions. WT cells subjected to 24 hours of hypoxia followed by 6 hours of reoxygenation had a loss of viability, whereas hypoxia/reoxygenation had no effect on *Trpm2*-KO PTCs. *Trpm2*-KO PTCs

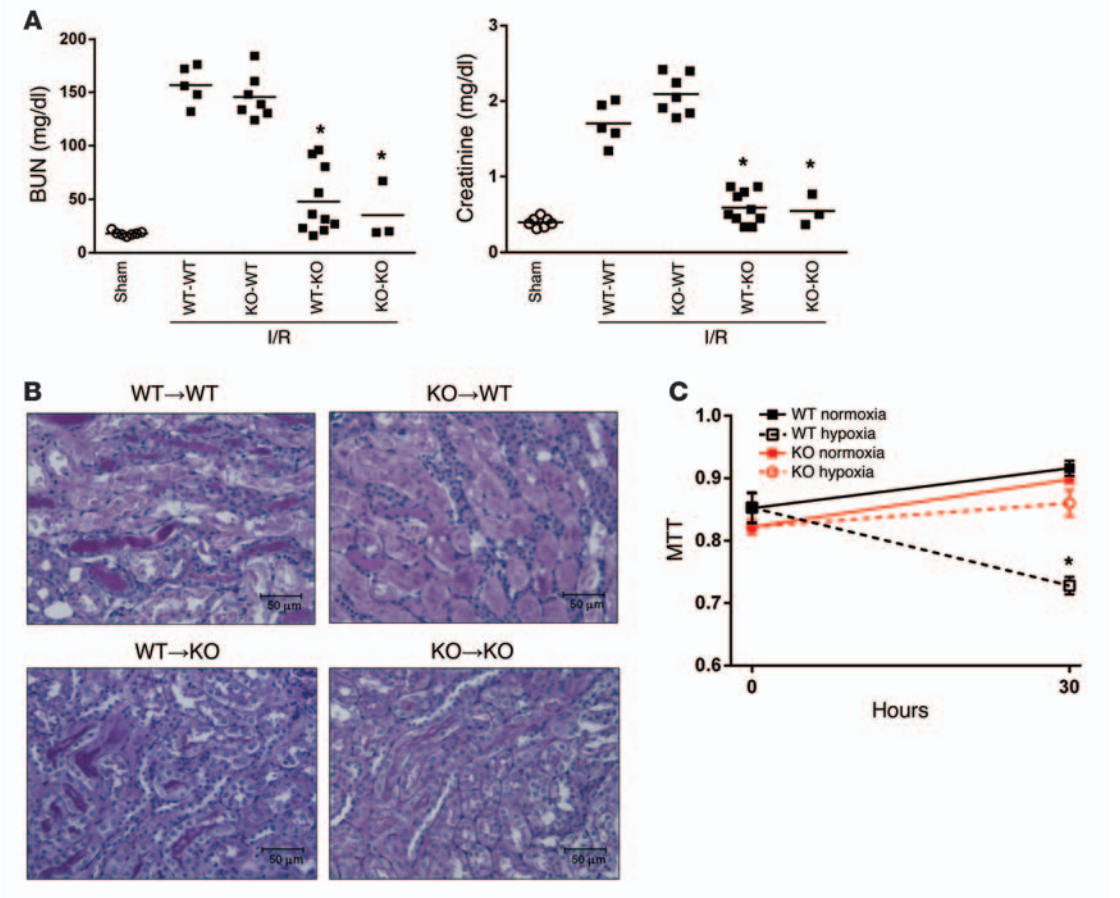

Figure 3. Parenchymal TRPM2 mediates ischemic AKI. (**A**) Chimeric mice were generated and subjected to kidney ischemia or sham surgery. Blood collected 24 hours after I/R was analyzed for BUN and serum creatinine. *$P < 0.001$ versus WT-WT. (**B**) PAS-stained kidney tissue sections. Scale bars: 50 μm. (**C**) Cell viability of primary cultured PTCs from WT or KO mice subjected to hypoxia/reoxygenation in vitro. *$P < 0.01$ versus normoxia.

were also more resistant than WT cells to oxidant-induced cell death in vitro (Supplemental Figure 6). These results support the view that TRPM2 expressed by kidney epithelial cells mediates ischemic or hypoxic injury.

Trpm2-KO mice are resistant to I/R-induced kidney parenchymal cell apoptosis. Kidney I/R is known to induce apoptosis of kidney tubular epithelial cells (37). We have previously demonstrated that TRPM2 is important in oxidant stress–induced apoptosis in vitro (16), but its role in apoptosis in vivo is unknown. TUNEL staining revealed no apoptotic cells in kidneys from sham WT or *Trpm2*-KO mice (Figure 4, A and B). However, I/R induced significant apoptosis in WT kidneys 24 hours after reperfusion. The apoptotic cells were almost exclusively kidney tubular epithelial cells. In contrast, we found that much less apoptosis was induced by I/R in *Trpm2*-KO kidneys. Likewise, we found that cleavage of poly(ADP-ribose) polymerase (PARP), activation of caspase 9, and activation of caspase 3 by ischemia were all attenuated in *Trpm2*-KO mice (Figure 4, C and D). In contrast, expression of the antiapoptotic proteins BCL-2 and BCL-X_L (Figure 4C) were higher in TRPM2-deficient mice than in WT mice.

Trpm2-KO mice have less RAC1-dependent oxidant stress after I/R. Oxidant stress contributes to ischemic kidney injury (38). To determine whether TRPM2 impacts kidney injury via oxidant stress, we measured 4-hydroxynonenal (4-HNE) adducts of proteins in kidneys from WT and *Trpm2*-KO mice. As shown in Figure 5A, I/R resulted in a large increase in 4-HNE adducts in WT mouse kidneys, but noticeably lower levels of 4-HNE signals in *Trpm2*-KO mice. Similarly, NADPH oxidase activity was markedly stimulated after I/R in WT mice, but was stimulated to a lesser extent in *Trpm2*-KO mice (Figure 5B).

RAC1 is an important determinant of NAPDH oxidase activation (39), hence, we determined the activity of RAC1 in mouse kidneys subjected to I/R injury. I/R led to a robust activation of RAC1, as reflected by GTP-bound RAC1, in kidneys of WT mice but resulted in less activity in *Trpm2*-KO kidneys (Figure 5C). To confirm that TRPM2 contributes to RAC1 activation, we measured RAC1 activity in primary cultured PTCs. As shown in Figure 5D, treatment of WT cells with H_2O_2 increased RAC1 activation. However, H_2O_2 treatment had little effect on RAC1 activity in *Trpm2*-KO cells. These results suggest that TRPM2 is required for oxidative stress–induced RAC1 activation.

Active RAC1 interacts with TRPM2 in an oxidant-dependent manner to increase membrane localization. Since TRPM2 is required for oxidative stress–induced RAC1 activation, we next determined whether TRPM2 interacts with RAC1. IP studies were performed in HEK293 cells transiently transfected with TRPM2 and RAC1. As shown in Figure 6A, pull-down of TRPM2 yielded RAC1 in the complex. Conversely, pull-down of RAC1 yielded

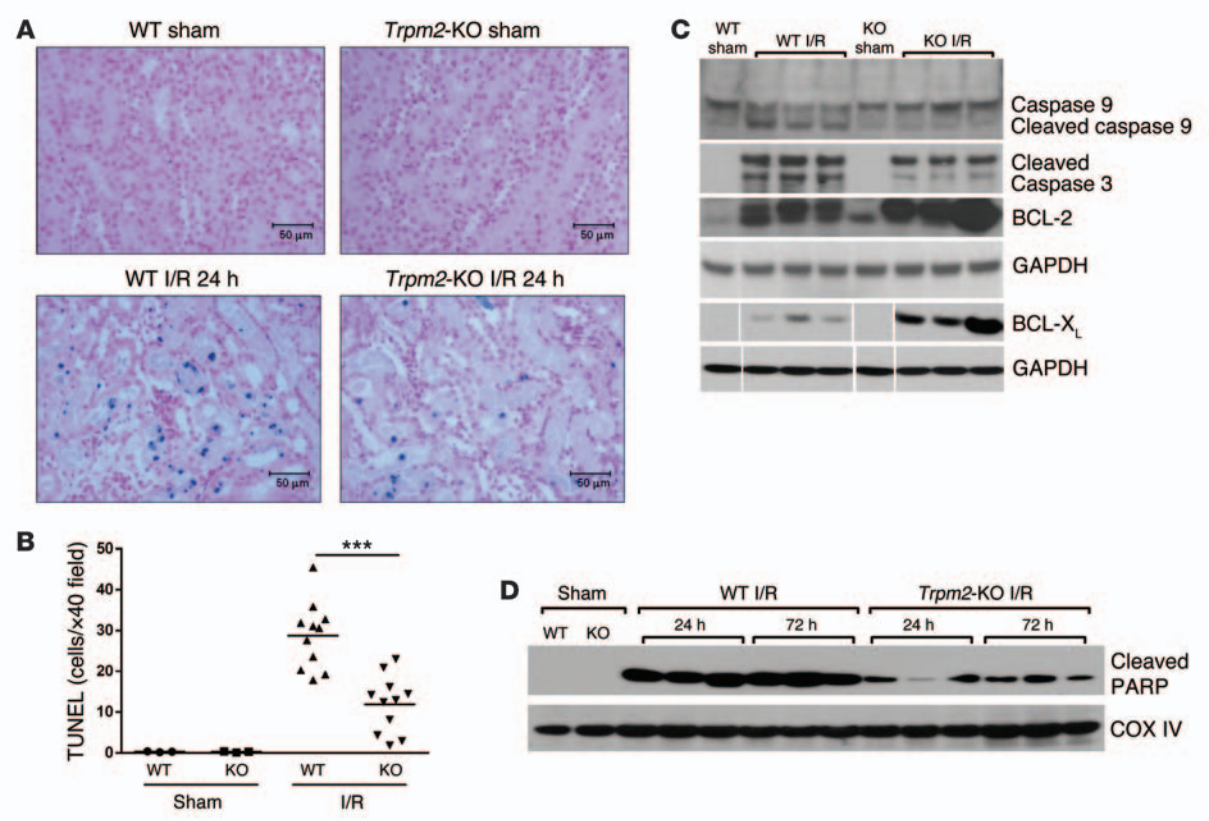

Figure 4. Reduction of epithelial cell apoptosis in *Trpm2*-KO mice. (**A**) TUNEL staining of kidney sections from *Trpm2*-KO and WT mice subjected to bilateral kidney ischemia or sham surgery. (**B**) Quantitation of apoptotic cells. ***$P < 0.001$. Scale bars: 50 μm. (**C**) Western blot analysis of kidney lysates from *Trpm2*-KO and WT mice subjected to bilateral kidney ischemia or sham surgery to detect pro- and antiapoptotic proteins. (**D**) Western blot analysis of PARP cleavage as a measure of apoptosis.

TRPM2 in the complex. H_2O_2 treatment enhanced this interaction dramatically (Figure 6B). Since H_2O_2 activates RAC1, we used DN and constitutively active (CA) RAC1 mutants to determine whether RAC1 activity is required for RAC1-TRPM2 interactions. Indeed, CA-RAC1 formed more complexes with TRPM2 than did DN-RAC1, even in the presence of H_2O_2, and the interaction of WT-RAC1, but not CA-RAC1, with TRPM2 was enhanced by H_2O_2 (Figure 6C). To determine whether TRPM2-RAC1 interactions occur in vivo, we pulled down active RAC1 using either a RAC1 Ab or PBD agarose and probed the complex for TRPM2 (Figure 6D). Although TRPM2 did not associate with RAC1 in sham kidneys (when RAC1 activity was low), there was interaction after I/R (Figure 6D), when the activity of RAC 1 was high (Figure 5C). Likewise, immunofluorescence localization of RAC1 and TRPM2 showed no overlap in proximal tubules from sham kidneys (Figure 6E). After I/R, TRPM2 staining became more punctate (as seen in Figure 1) and demonstrated colocalization with RAC1 (Figure 6E). RAC1 has been shown to regulate the trafficking of TRPC5 (40). We performed surface biotinylation studies to determine whether RAC1 alters the membrane localization of TRPM2. We found that H_2O_2 increased the biotinylation of TRPM2, and this effect was abolished by DN RAC1 (Figure 7). CA RAC1 increased TRPM2 surface biotinylation even in the absence of H_2O_2. These results suggest that RAC1 physically interacts with TRPM2 to increase its membrane localization, and this interaction is increased in the setting of oxidative stress through the activation of RAC1.

Inhibition of RAC1 protects against kidney I/R injury in vivo. Although we documented an increase in RAC1 activity in kidneys after I/R and an interaction between RAC1 and TRPM2, the role of RAC1 in mediating I/R kidney injury has not been reported. To determine the functional significance of such RAC1 activation, we treated mice with NSC23766, a potent and specific inhibitor of RAC1 activation (41, 42), prior to ischemic injury. As shown in Figure 8A, the NSC23766-treated mice had better preservation of kidney function than did vehicle-treated mice. NSC23766 had no additive effects on kidney function in *Trpm2*-KO mice. NSC23766 reduced PARP cleavage and caspase 3 activation and increased BCL-2 in kidneys subjected to I/R (Figure 8B). We found that oxidative stress measured by 4-HNE adducts (Figure 8C) was reduced in the kidneys of WT mice treated with the RAC1 inhibitor to the levels seen in *Trpm2*-KO mice. Likewise, thiobarbiturate reactive substances (TBARS), another measure of oxidative stress, were higher in WT kidneys subjected to I/R than in *Trpm2*-KO kidneys (Figure 8D), and treatment of WT mice with the RAC1 inhibitor reduced TBARS levels to those seen in *Trpm2*-KO mice. Finally, NADPH oxidase activity was reduced in kidneys of NSC23766-treated mice (Figure 8E). These results demonstrate that RAC1 plays an important role in kidney I/R injury and in the generation of oxidant stress during kidney ischemia. They also provide further evidence that TRPM2 contributes to kidney I/R injury by increasing activation of RAC1.

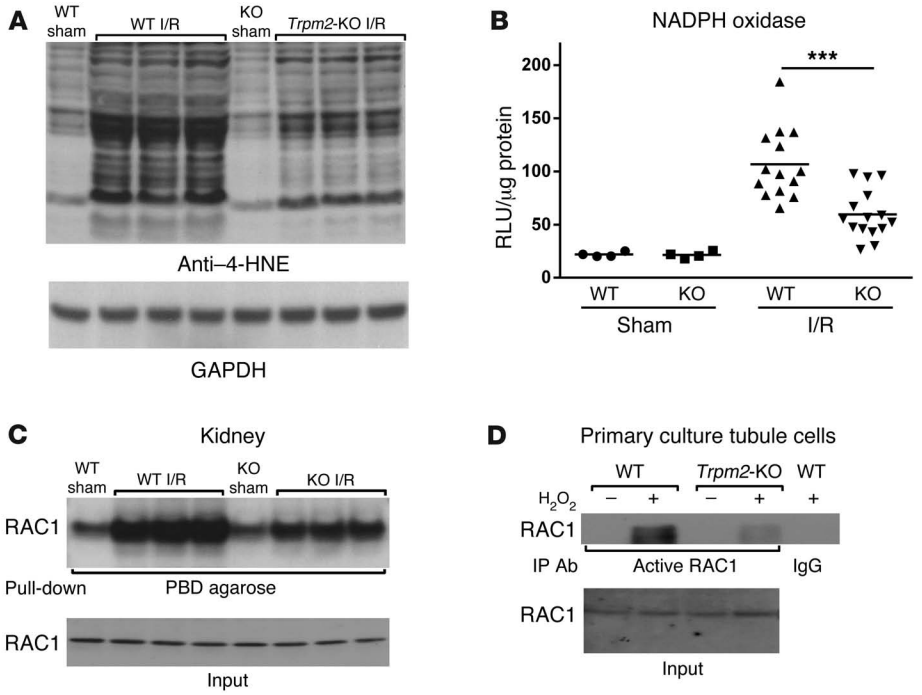

Figure 5. Reduction of oxidative stress and RAC1 activation in *Trpm2*-KO mice. (**A**) Western blot analysis of 4-HNE adducts in kidney lysates from *Trpm2*-KO and WT mice subjected to bilateral kidney ischemia. The same gel used in Figure 4C was reprobed with a 4-HNE Ab. (**B**) NADPH oxidase activity in kidney lysates from WT and *Trpm2*-KO mice subjected to bilateral kidney ischemia followed by 6 hours of reperfusion. ***$P < 0.001$. (**C**) RAC1 activity in kidney lysates from WT and *Trpm2*-KO mice subjected to ischemia or sham surgery. (**D**) RAC1 activity in primary kidney PTCs after H_2O_2 treatment.

Discussion

The present study examined the role of TRPM2, a transient receptor potential (TRP) channel, as a mediator of ischemic AKI. A number of previous studies have reported that TRPM2 is capable of sensing and responding to oxidative stress and that it plays a critical role in cell proliferation and oxidant-induced cell death in vitro (16, 23). However, the role of TRPM2 in disease processes in vivo is poorly understood due to the lack of specific inhibitors and the only recent development of KO models (43–45). Nonetheless, TRPM2 has several features that make it an attractive candidate to mediate ischemic AKI. For example, TRPM2 is activated by oxidant stress, intracellular calcium, ADPR, and TNF-α (20–23), all of which are known to be increased in ischemic AKI (24, 25). Conversely, TRPM2 is inhibited by low temperature and acidosis, both of which reduce ischemic AKI (46, 47). We explored the role of TRPM2 in AKI in vivo using a newly developed *Trpm2*-KO mouse (43). Our studies yielded several important findings.

First, although previous studies using a variety of ion channel antagonists in mainly in vitro settings have implicated potassium (6, 11, 48), chloride (7–9), and calcium channels (10) in the pathogenesis of ischemic or toxic kidney injury, the molecular identity and in vivo relevance of any such channel has been undefined. Here, we demonstrated, using both in vivo and in vitro models and genetic and pharmacologic approaches, that TRPM2 is a critical mediator of I/R-induced kidney dysfunction, histologic injury, kidney epithelial cell apoptosis, oxidant stress, and kidney neutrophil infiltration. Moreover, inhibition of TRPM2 up to 6 hours after the ischemic insult still afforded some protection from injury (Supplemental Figure 3). This window of opportunity might allow for greater translational potential, since ischemic insults are not always predictable clinically.

Ischemic kidney injury is characterized by decreases in potassium and increases in cellular sodium, calcium, and cell volume (3, 4). We also found decreases in tissue potassium and increases in calcium after ischemia (Table 1). Although the changes in electrolyte content were smaller in *Trpm2*-KO mice than in WT mice, these differences were not statistically significant. Earlier work indicated that the electrolyte content of kidney epithelial cells is largely repaired within 2 hours after reperfusion (4). Thus, our measurements at 6 hours may have underestimated the role of TRPM2 in ischemia-induced electrolyte dysregulation. At present, it is unclear whether TRPM2 is directly responsible for calcium influx and potassium leak during ischemia. We did not see localization of TRPM2 in the plasma membrane in kidney epithelial cells. After ischemia, TRPM2 appeared to move to intracellular organelles. TRPM2 expressed in lysosomes controls intracellular calcium release in dendritic cells and pancreatic β cells (36, 49). Thus, it is possible that TRPM2 affects injury in PTCs at intracellular loci, such as mitochondria or lysosomes, rather than through ion transport into the cell (50).

There are few studies of TRPM2 in ischemic injury involving other tissues. Jia et al. showed protection from ischemic stroke using another TRPM2 inhibitor, clotrimazole, or TRPM2 siRNA in mice (51). 2-APB was also reported to decrease liver ischemic injury, though the pathway involved was not defined (52). Studies of TRPM2 in myocardial ischemia have yielded conflicting results. Using a different TRPM2-deficient mouse, Hiroi et al. reported that TRPM2-deficient mice were protected against I/R injury induced by occlusion of the left main coronary artery (44). These effects, however, were attributed to TRPM2 expression in neutrophils, whereas our studies using bone marrow chimeras (Figure 3) clearly show that the effects of TRPM2 in kidney ischemia are mediated by radioresistant cells rather than neutrophils. The conclusions in the Hiroi study were based on ex vivo studies that did not specifically determine the role of neutrophils in vivo (44). In contrast, using the same mice as in the

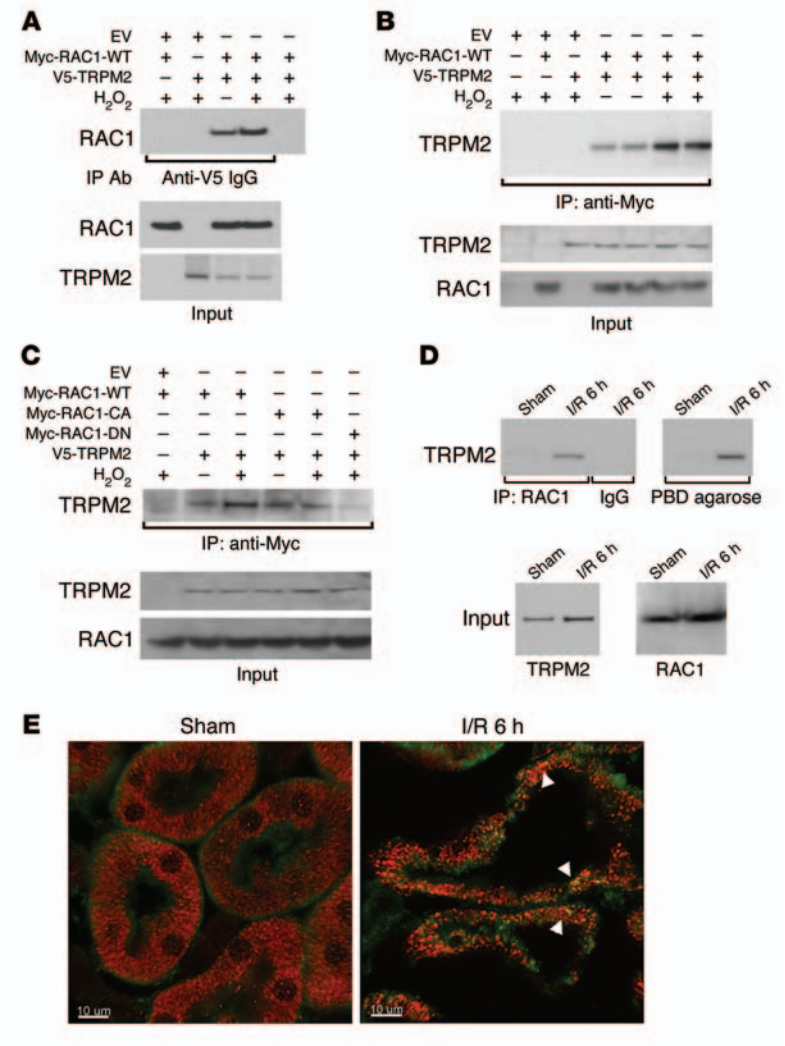

Figure 6. TRPM2 interacts with active RAC1. (**A**) HEK293 cells were transiently transfected with TRPM2 with an N-terminal V5 Tag and RAC1 with an N-terminal Myc Tag. Top panel: IP of TRPM2 using anti-V5 and immunoblot of RAC1 using anti-Myc Ab. Bottom panels: Equal expression of transfected Myc-RAC1 and V5-TRPM2 in the cell lysates. (**B**) Transfected cells were treated with H_2O_2 prior to lysis. Lysates were subjected to IP of RAC1 using anti-Myc Ab followed by immunoblotting for TRPM2. (**C**) HEK293 cells were transiently transfected with V5-TRPM2 and either Myc-RAC1-WT, Myc-RAC1-CA, or Myc-RAC1-DN. After H_2O_2 treatment, cells were lysed, followed by IP with anti-Myc Ab and immunoblotting with anti-V5 Ab. EV, empty vector. (**D**) Pull-down of active RAC1 from kidneys subjected to sham surgery or I/R using a RAC1 Ab (left) or PBD agarose (right), with immunoblotting for TRPM2. (**E**) Merged confocal images of TRPM2 (red) and RAC1 (green) in kidneys subjected to sham or I/R surgery. Arrowheads denote areas of overlap (yellow). Scale bars: 10 μm.

present study, Miller et al. (43) found that an absence of TRPM2 exacerbated myocardial ischemic injury and increased oxidative stress, whereas we found a reduction in both ischemic injury and oxidative stress in the kidney. The reasons underlying the differential responses to coronary versus kidney ischemia in the same *Trpm2*-KO mouse are not clear but may relate to different functions for ion channels and intracellular calcium regulation in epithelia and excitable tissues. In a similar vein, inhibitors of K_{ATP} channels are reported to have a beneficial impact on ischemic kidney epithelial cells (6, 11) but exacerbate myocardial ischemic injury (53). Certainly, differences in the expression of a variety of proteins and the resulting dissimilar intracellular environments may also contribute to the different responses.

Several lines of evidence suggest that TRPM2 in kidney epithelial cells is responsible for its effects during ischemic AKI. First, we localized TRPM2 within the kidney to the proximal tubule epithelial cell. Second, chimeric mice, which expressed TRPM2 in the kidney but not in bone marrow–derived cells, were susceptible to ischemic AKI, whereas mice expressing TRPM2 in bone marrow–derived cells but not in the kidney were resistant to ischemic AKI. Third, apoptosis of kidney tubular epithelial cells was reduced in TRPM2-deficient mice in vivo. Fourth, cultured kidney epithelial cells displayed TRPM2-dependent cell death in response to hypoxia in vitro. Endothelial cell dysfunction is a mediator of AKI (54). Studies have clearly demonstrated both the presence, by Western blot analysis, and the functional activity of TRPM2 within endothelial cells, where it mediates apoptosis and vascular permeability in response to oxidant stress (14, 55). Although we did not see TRPM2 expression in kidney endothelial cells (Figure 1), it is possible that low levels of expression, which are still functionally relevant, were not detected by our immunofluorescence microscope studies. Accordingly, our results do not exclude the possibility that TRPM2 in endothelial cells, or at other sites, could mediate ischemic AKI in vivo. Further studies using tissue-specific TRPM2 deletion will be required to address this issue.

Oxidant stress is a known activator of TRPM2 (23). Our finding that TRPM2 activation results in increased oxidant stress provides a possible positive feedback loop, wherein oxidant stress activates TRPM2, resulting in additional oxidant stress. ADPR is also a potent activator of TRPM2 by binding to the nudix-like domain in the C terminus of TRPM2 (56). PARP is activated by oxidant stress (57) and ischemia (58). Inhibition of PARP reduces oxidant-induced cell death in kidney epithelial cells in vitro (57) and preserves kidney function after ischemic insults in vivo (58, 59). Since the sequential activity of PARP and poly(ADP-ribose) glycohydrolase (PARG) produces ADPR (56), it is possible that ADPR is an important activator of TRPM2 during ischemia. As a corollary, the salutary effects of PARP inhibitors in ischemic AKI may be due to less ADPR production and a subsequent reduction in TRPM2 activation.

We provide clear evidence that TRPM2 contributes to ischemia-induced apoptosis in vivo. The reduced activity of caspase 9 in *Trpm2*-KO mice suggests that TRPM2 promotes mitochondrial pathways of apoptosis. Likewise, the observed increase in BCL-2 and BCL-X_L expression in the TRPM2-deficient mice may account for suppression of mitochondrial apoptosis. In this regard, BCL-2 expression increases after kidney ischemia (60) and overexpression of BCL-2 reduces kidney ischemic injury (61, 62). Increases in intracellular calcium (63) and oxidant stress (64) are triggers for apoptosis. Accordingly, a reduction in TRPM2-dependent calcium entry or release from intracellular stores (36, 49) or the reduction

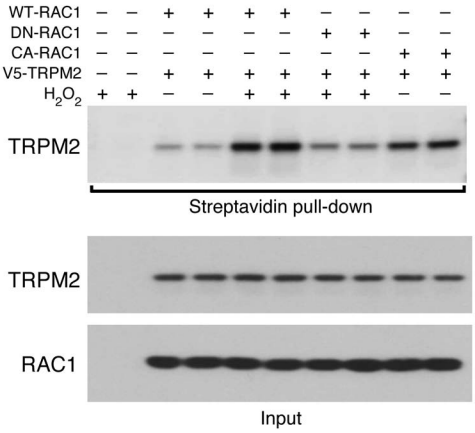

Figure 7. H_2O_2 increases membrane expression of TRPM2 by activation of RAC1. HEK293 cells were transiently transfected with V5-TRPM2 and either Myc-RAC1-WT, Myc-RAC1-CA, or Myc-RAC1-DN and then treated with H_2O_2 or vehicle. After H_2O_2 treatment, cell surface biotinylation was performed. Biotinylated proteins were isolated using streptavidin beads followed by Western blotting with anti-V5 Ab to identify biotinylated TRPM2 (top panel). Total TRPM2 and RAC1 content in the cell lysate is shown in the lower panels.

in oxidant stress we observed may also contribute to less apoptosis. This is supported by in vitro observations that overexpression of TRPM2 sensitizes cells to apoptosis induced by oxidant stress (16), while expression of a DN TRPM2 inhibits calcium entry and apoptosis in HEK293 cells (15). Likewise, a recent study demonstrated that oxidant stress alters the interactions between TRPM2 and the inhibitory splice variant TRPM2-S in endothelial cells, resulting in TRPM2 activation, increased calcium entry, and subsequent apoptosis (14). The role of TRPM2 splice variants in ischemic tissue injury warrants further investigation.

We also found that RAC1 is activated after kidney ischemia. Previous work on RAC1 in kidney disease has focused on its role in the podocyte, where unrestrained activation of RAC1 leads to podocyte effacement and proteinuria (65–68) and kidney fibrosis, whereby RAC1 alters macrophage migration (69). In contrast, the role of RAC1 in AKI has received little attention. Using an inhibitor of RAC1 activation, we determined that RAC1 plays an important role in ischemic kidney injury. A role for RAC1 has also been reported in ischemic injury of the liver (70), heart (71), and brain (72). RAC1 exerts a wide range of cellular effects, including regulation of the production of ROS (27). RAC1 recruits subunits of the NADPH oxidase complex to increase ROS production (39). Indeed, we found that inhibition of RAC1 results in reduced NAPDH oxidase activity, less oxidant stress and apoptosis, and better preservation of kidney function, supporting the view that RAC1 contributes to ischemic AKI, at least in part, through an increase in ROS production. Other mechanisms, such as altering the actin cytoskeleton, may also be operative. Regardless of the mechanism, our results indicate that RAC1 may be a novel target for the prevention of ischemic AKI.

The observations that RAC1 activity is TRPM2 dependent, that TRPM2-deficient mice exhibit less oxidant stress and lower levels of NADPH oxidase activity in response to ischemia than do WT mice, that RAC1 inhibition reduces oxidant stress to the levels seen in TRPM2-deficient mice, and that the RAC1 inhibitor had no added effect in TRPM2-deficient mice all suggest that TRPM2 increases oxidant stress through the activation of RAC1 and, subsequently, NADPH oxidase. A different role for TRPM2 has been proposed for oxidant production in neutrophils. Specifically, in neutrophils, TRPM2 reduced LPS-induced oxidant production by depolarizing the plasma membrane, thereby reducing NADPH oxidase activity (45). It is possible that TRPM2 both stimulates NADPH oxidase via RAC1 and inhibits NADPH oxidase through its effects on membrane voltage, with the net effect determined by a cell- and stimulus-dependent balance. In neutrophils, since LPS activates NADPH oxidase via RAC1 (73), the inhibitory effect of TRPM2 via depolarization may predominate. In kidney cells, the stimulatory effect of TRPM2 through RAC1 activation may predominate. We did not directly examine the role of NADPH oxidase in kidney I/R, though apocynin, an NADPH oxidase inhibitor, is reported to decrease kidney ischemic injury (74). Further studies will be needed to define the isoforms and location of NADPH oxidase relevant to ischemic kidney injury.

Our results also uncovered a bidirectional interaction between TRPM2 and RAC1. We determined that TRPM2 is required for RAC1 activation in response to either ischemia in vivo or oxidant stress in vitro. Co-IP studies indicated that TRPM2 and RAC1 form a complex and that this complex formation is enhanced by the activation of RAC1 both in vitro and in vivo. The presence of active RAC1 also increased the plasma membrane localization of TRPM2 in vitro. We did not observe plasma membrane localization in vivo, but speculate that RAC1 facilitates TRPM2 trafficking to intracellular membranes. This scenario, wherein TRPM2 activates RAC1 and active RAC1 increases membrane delivery of TRPM2, is highly analogous to the interactions between another TRP channel, TRPC5, and RAC1 in podocytes. Studies by Greka et al. have shown that TRPC5-mediated calcium influx is required for RAC1 activation in response to angiotensin II in podocytes (75) and that RAC1 increases trafficking of TRPC5 to the plasma membrane (40). Moreover, just as inhibition of TRPM2 reduces kidney injury in response to ischemia, inhibition of TRPC5 reduces proteinuria in response to protamine sulfate or LPS (76).

In summary, we demonstrate that TRPM2 is a critical mediator of ischemic AKI. The mechanism whereby TRPM2 promotes AKI, though not fully defined, involves the activation of RAC1 and subsequent oxidative stress and the activation of mitochondrial apoptotic pathways. RAC1 physically interacts with TRPM2 and increases its membrane localization. The TRPM2-RAC1 interactions are favored by active RAC1. RAC1 also increases NADPH oxidase activity in the ischemic kidney. Since oxidative stress activates TRPM2, a positive feedback loop may be initiated, in which oxidant stress activates TRPM2 and subsequent RAC1 activation, leading to greater membrane TRPM2 levels and greater oxidant injury. Pharmacologic inhibition of either TRPM2 or RAC1 was

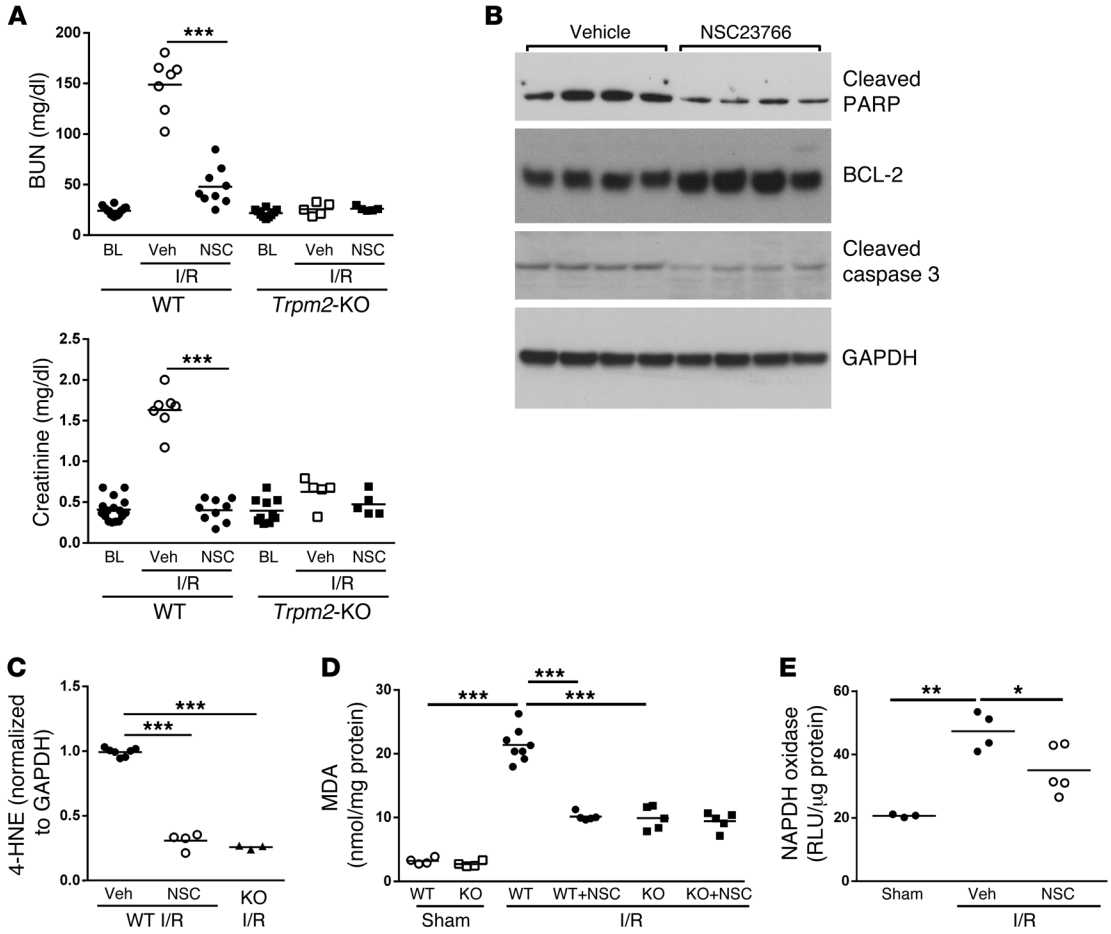

Figure 8. Pharmacological blockade of RAC1 protects against ischemic AKI. (**A**) WT (circles) or MDA (squares) mice were pretreated with RAC1 inhibitor NSC23766 (NSC) (black symbols) or vehicle (Veh) (white symbols) and subjected to bilateral kidney ischemia. BUN and serum creatinine levels prior to (BL) and 24 hours after I/R.(**B**) Western blot analysis of kidney lysates from WT and *Trpm2*-KO mice 24 hours after I/R using Abs against cleaved PARP, BCL-2, caspase 3, and GAPDH. (**C**) Densitometric analysis of Western blotting of kidney lysates using anti–4-HNE. (**D**) TBARs (MDA) in kidney tissues from *Trpm2*-KO and WT mice. (**E**) NADPH oxidase activity in WT mice subjected to sham or I/R in the presence or absence of NSC23766. $^{*}P < 0.05$; $^{**}P < 0.01$; $^{***}P < 0.001$.

also shown to greatly reduce the severity of ischemic AKI in vivo. Therefore, targeting either TRPM2 or RAC1 may be effective strategies to prevent or reduce ischemic kidney injury.

Methods

Reagents. 2-APB and NSC23766 were purchased from Sigma-Aldrich and Tocris, respectively. Plasmid pRK5-Myc-RAC1-T17N (Addgene plasmid 12984, deposited by the late Gary Bokoch, The Scripps Research Institute, La Jolla, California, USA) was obtained from Addgene.org. Other Myc-RAC1 plasmids were provided by Lorraine Santy (The Pennsylvania State University, University Park, Pennsylvania, USA), and V5-TRPM2 in pcDNA3.1 was described previously (15). The following Abs were used: TRPM2 (Aviva Systems Biology); BCL-2 and BCL-XL (Santa Cruz Biotechnology Inc.); GAPDH, PARP (cleaved), COX IV, β-tubulin, caspase 3, caspase 9, HRP-conjugated goat anti-mouse, and goat anti-rabbit (Cell Signaling Technology); anti-V5, anti-Myc, Alexa Fluor 594–conjugated goat anti-rabbit Ab, and Alexa Fluor 488–conjugated goat anti-mouse Ab (Invitrogen); total RAC1 (EMD Millipore); RAC1-GTP (NewEast Biosciences); and 4-HNE (Abcam). The RAC1 activity assay kit was purchased from EMD Millipore.

TRPM2-deficient mice. *Trpm2*-KO mice were generated on a C57BL/6 background (43). WT C57BL/6 littermates were used as control mice in the initial experiments, but C57BL/6 mice purchased from The Jackson Laboratory were used in the majority of experiments. Experiments were performed on 7- to 8-week-old mice, except chimeric mice, which were 14 weeks of age.

Creation of chimeric mice. Chimeric mice were created using *Trpm2*-KO mice and WT mice as either bone marrow donors or recipients, as described previously (77). Four sets of chimeric mice were created: WT→WT (WT donor and recipient); WT→KO (WT donor and TRPM2 KO recipient); KO→WT (*Trpm2*-KO donor and WT recipient); and KO→KO (*Trpm2*-KO donor and recipient). PCR of genomic DNA isolated from peripheral blood confirmed that over 95% of the circulating leukocytes in the chimeras were of donor origin (Supplemental Figure 7).

Induction of ischemic AKI. *Trpm2*-KO mice or control WT mice (7–8 weeks of age) and chimeric mice (8 weeks after bone marrow transfer), were anesthetized with sodium pentobarbital (50 mg/kg BW) i.p. and were placed on a heating pad to maintain core temperature at 37°C, as previously performed in our laboratory (29, 30). Both kidney pedicles were identified through dorsal incisions and clamped

for 28 minutes. Control animals were subjected to the same surgical procedure but did not have their kidney pedicles clamped. 2-APB (16 mg/kg BW in 10% DMSO and 90% saline) and NSC23766 (10 mg/kg BW in saline) were injected i.p. 1 hour before surgery, when needed. At the time of sacrifice, kidneys were cut in half longitudinally, half of 1 kidney from each mouse was fixed in buffered 10% formalin for histologic analysis. The remaining kidney tissues were snap-frozen in liquid nitrogen and stored at –80°C.

Kidney function. BUN (VITROS DT60II Analyzer; Ortho Clinical Diagnostics) and serum creatinine (DZ072B; Diazyme Laboratories) were measured as described previously (29, 30). Key serum creatinine results were confirmed using a liquid chromatography tandem-mass spectrometry (LC-MS/MS) method (Supplemental Figure 8).

Histological analyses. Kidney tissue was fixed in buffered 10% formalin for 12 hours and then embedded in paraffin wax. For assessment of injury, 5-μm sections were stained with periodic acid Schiff (PAS). Acute tubular injury was assessed in the outer stripe of the outer medulla and inner cortex using a semiquantitative scale (78, 79). To quantitate neutrophil infiltration, sections were stained with rat anti-mouse neutrophil Ab (1:200 dilution; Serotech). Apoptotic cells were detected by terminal deoxynucleotidyl transferase–mediated (TdT-mediated) TUNEL using an In Situ Apoptosis Detection Kit (R&D Systems) according to the manufacturer's instructions. The individuals examining the slides for histology, neutrophil infiltration, and apoptotic cell quantity were blinded to the genotypes and treatment of the mice.

Immunofluorescence microscopy. TRPM2 and RAC1 were localized by immunofluorescence of paraformaldehyde-fixed frozen sections as described before (80), with modification. Sections (6-μm-thick) were permeabilized with 0.3% Triton X-100 in PBS, washed, and blocked with 10% goat serum containing 2% BSA. The sections were incubated overnight with a rabbit TRPM2 polyclonal Ab (1:200 dilution, catalog ARP44380_P050; Aviva Systems Biology) that recognizes both the full-length and short isoform of TRPM2 and/or a mouse RAC1 mAb (1:200 dilution, catalog 610652; BD Transduction Laboratories). Primary Abs were detected using Alexa Fluor 594– and Alexa Fluor 488–conjugated goat anti-rabbit and anti-mouse Abs, respectively. Brush borders of proximal tubules were visualized with FITC-labeled LTL (1:400; Vector Laboratories). Slides were mounted in aqueous mounting medium containing DAPI. Images were collected with a Leica TCS SP8 confocal microscope, and Imaris Image Analysis software was used. Sections stained without incubation with the TRPM2 Ab and sections from TRPM2-deficient mice served as negative controls for the immunostaining.

Flow cytometry. Kidneys were digested with collagenase D (2 mg/ml) and DNase I (15 U/ml) for 30 minutes as described previously (81, 82). The digested kidney suspension was passed through 100-μm mesh and then 40-μm mesh. Kidney cells were stained for leukocytes and neutrophils using anti-CD45 (30-F11) and Ly6G (1A8) Abs, respectively. Flow cytometry was performed on a FACSCalibur cytometer (BD Biosciences) and analyzed using FlowJo software (Tree Star Inc.).

Calcium and potassium content of kidney. Kidneys were harvested 6 hours after a 28-minute period of ischemia and immediately frozen in liquid nitrogen. Portions of kidney cortex were weighed and digested in HPLC-grade nitric acid (10:1 volume/weight ratio) at 80°C for 1 hour with frequent vortexing. The digest was centrifuged at 10,000 *g* for 5 minutes. The supernatant was diluted in deionized water (1:100 for potassium and 1:20 for calcium) and analyzed by atomic absorption spectroscopy (AAnalyst 800; PerkinElmer) at the Water Quality Laboratory of the Penn State Institutes of Energy and the Environment.

Western blot analysis. The frozen kidney tissues were homogenized in lysis buffer (20 mM Tris [pH 7.5], 1% Triton X-100, 10% glycerol, 137 mM NaCl, 2 mM EDTA, 25 mM glycerophosphate, 1 mM Na_3VO_4, and protease inhibitor cocktail) (Roche Applied Science). The lysates were centrifuged at 14,000 *g* for 15 minutes at 4°C, and the supernatants were transferred to new tubes. Samples (30-μg) of total protein were separated on 4% to 12% NuPAGE (Invitrogen), transferred to a polyvinylidene fluoride membrane, and blotted with primary (overnight) then secondary (1 hour) Abs. Proteins were detected using ECL reagents (Thermo Scientific).

Quantitation of mRNA by real-time RT-PCR. Real-time RT-PCR was performed in a CFX96 Touch real-time PCR detection system (Bio-Rad). RNA was isolated from kidneys using TRIzol reagent (Invitrogen). Total RNA (2.0 μg) was reverse transcribed in a reaction volume of 20 μl using an Omniscript RT Kit (QIAGEN) and random primers. The product was diluted to a volume of 110-μl and 1-μl aliquots, which were used as templates for amplification using SYBR Green PCR amplification reagent (QIAGEN) and the following gene-specific primers: TRPM2, forward: 5′-GACATTGTCCGGAGGCGGCA-3′, reverse: 5′-GCGATGTCCACGCGGTTCCA-3′; NGAL, forward: 5′-AATGTCACCTCCATCCTGGTC-3′, reverse: 5′-GCCACTTGCACATTGTAGCTC-3′; and GAPDH, forward: 5′-TCCCAGACCCCATAACAACAG-3′, reverse: 5′-TGAGGGTGCAGCGAACTTTA-3′.

RAC1 activity assay. Snap-frozen kidney tissues were homogenized on ice in Mg^{2+} lysis buffer containing 25 mM HEPES (pH 7.5), 150 mM NaCl, 1% igepal CA-630, 10 mM $MgCl_2$, 1 mM EDTA, and 10% glycerol, with 1 mM Na_3VO_4, protease inhibitor cocktail, and phosphatase inhibitors (Sigma-Aldrich). Cultured cells were washed with prewarmed PBS and incubated in PBS for 1 hour followed by 1 mM H_2O_2 treatment for 5 minutes. The cells were then immediately washed with ice-cold PBS and lysed in Mg^{2+} lysis buffer. Lysates were centrifuged at 14,000 *g* at 4°C for 15 minutes, and the protein concentration was determined by BCA protein assay. Samples (1,000-μg) of lysate protein were mixed with either an Ab that only detected active, GTP-bound RAC1 or PAK-1 PBD agarose beads (Millipore) to bind active RAC1. Bound proteins were washed 3 times in lysis buffer. After the final wash, the pellets were subjected to Western blot analysis using a RAC1 Ab.

Co-IP and cell surface biotinylation. HEK293 cells were maintained in DMEM supplemented with 10% FBS at 37°C and 95% air-5% CO_2 in a standard humidified incubator. HEK293 cells were transiently transfected with empty plasmids (EV) or plasmids encoding V5-tagged TRPM2, Myc-RAC1, or V5-TRPM2 plus Myc-RAC1 using X-tremeGENE HP DNA transfection reagent (Roche). Twenty-four hours later, the transfected cells were washed with warm PBS followed by 1 mM H_2O_2 treatment for 5 minutes. The cells were then placed on ice, washed with ice-cold PBS, then lysed in Mg^{2+} lysis buffer. Protein lysate samples (1,000-μg) were mixed with 1 μg V5 or Myc Ab at 4°C on a rocking platform for 2 hours, followed by protein A/G-Plus agarose beads (Santa Cruz Biotechnology Inc.) for 1 hour, then 3 washes with 500 μl lysis buffer. After the final wash, all supernatant was carefully removed, and pellets were kept at –20°C until ready for electrophoresis. Pull-down of RAC1 from kidney was performed by mixing 1,000 μg of kidney homogenate with either PBD agarose or RAC1-GTP Ab (2 μg) on a rocking platform at 4°C for 2 hours followed, for RAC1 Ab

samples, by protein A/G-Plus beads. Biotinylation of cell surface proteins was examined as described by Yu et al. (83).

Primary cell culture. PTCs were prepared under sterile conditions from collagenase-digested cortical fragments of kidneys isolated from 8-week-old *Trpm2*-KO and WT mice as described by Terryn et al. (84). The PTCs were cultured in DMEM/F12 (supplemented with 1% heat-inactivated FCS, 50 nmol/l hydrocortisone, insulin-transferrin-selenium solution [1:100], nonessential amino acids [1:100], and penicillin-streptomycin solution [1:100] buffered to pH 7.4) at 37°C in a 95% air-5% CO_2 humidified incubator, and medium was replaced every 2 days. After 7 days, cells were subjected to hypoxia generated using the BD Bioscience GasPak EZ Anaerobe Pouch System (85). Cultured cells were placed inside the pouches and incubated at 37°C for 24 hours. Following hypoxia, the medium was changed to fresh, prewarmed DMEM/F12 primary culture medium, and cells were reoxygenated for 6 hours. Normoxic controls were subjected to 24 hours of normoxia, followed by a change of media and 6 hours of additional normoxia.

MTT assay. Primary cultured kidney PTCs were seeded in 96-well plates at a concentration of 1×10^5 cells per well in a 200-μl volume of growth medium. After the indicated treatment period, the supernatant was removed, and cells were washed 3 times with 1X PBS. Two hundred microliters of MTT reagent (0.5 mg/ml; Sigma-Aldrich) in medium was added to each well, and the plates were incubated for 4 hours at 37°C in a humidified incubator. The MTT reagent solution was removed from each well, and acidified methanol was added to dissolve the formazan salt. The absorbance at 570 nm was determined to quantify the formazan product present in each well. All assays were run at least in triplicate and repeated 3 times.

NADPH oxidase assay. NADPH oxidase activity was measured by the lucigenin-ECL method (86). Photon emission was measured in a luminometer. Photon emission in the absence of NADPH was subtracted to yield NADPH oxidase activity. The NADPH oxidase activity was normalized by the protein content and expressed in RLU/mg of protein.

Measurement of TBARs. The measurement of TBARS in the kidney was based on the formation of malondialdehyde (MDA) as described by Liu et al. (87).

Statistics. All assays were performed in duplicate or triplicate. Data are reported as the means ± SEM. Statistical significance was assessed by an unpaired, 2-tailed Student's *t* test for single comparison or by ANOVA for multiple comparisons. $P < 0.05$ was considered statistically significant. GraphPad Prism (GraphPad Software) was used for statistical analyses and graphs.

Study approval. All experiments involving mice were approved by the IACUC of the Penn State College of Medicine.

Acknowledgments

This work was supported by grants from the Genzyme Renal Innovations Program (to B.A. Miller and W.B. Reeves) and the NIH (DK081876, to W.B. Reeves). B.A. Miller was also supported by the Four Diamonds Fund of the Pennsylvania State University. N.E. Briley was supported by the AHA-SURF summer undergraduate research program (12UFEL10080000). M.I. Love was supported by the INTREPID summer undergraduate research program. We thank Lorraine Santy (The Pennsylvania State University) for providing RAC1 plasmids. We thank Dongxiao Sun (Penn State Mass Spectrometry Core) for performing LC-MS/MS measurements of creatinine. Confocal imaging was performed in the Microscopy Imaging Core Laboratory. The core facilities are funded, in part, by a grant from the Pennsylvania Department of Health using Tobacco CURE Funds. The Department specifically disclaims responsibility for any analyses, interpretations, or conclusions.

Address correspondence to: W. Brian Reeves, Division of Nephrology, Room C5830, Penn State College of Medicine, 500 University Drive, Hershey, Pennsylvania 17033, USA. Phone: 717.531.8156; E-mail: wreeves@psu.edu.

1. Nash K, Hafeez A, Hou S. Hospital-acquired renal insufficiency. *Am J Kidney Dis*. 2002;39(5):930–936.
2. Kosieradzki M, Rowiński W. Ischemia/reperfusion injury in kidney transplantation: mechanisms and prevention. *Transplant Proc*. 2008;40(10):3279–3288.
3. Mason J, Beck F, Dorge A, Rick R, Thurau K. Intracellular electrolyte composition following renal ischemia. *Kidney Int*. 1981;20(1):61–70.
4. Beck FX, Ohno A, Dorge A, Thurau K. Ischemia-induced changes in cell element composition and osmolyte contents of outer medulla. *Kidney Int*. 1995;48(2):449–457.
5. Leaf A. Cell swelling: A factor in ischemic tissue injury. *Circulation*. 1973;48(3):455–458.
6. Reeves WB, Shah SV. Activation of potassium channels contributes to hypoxic injury in proximal tubules. *J Clin Invest*. 1994;94(6):2289–2294.
7. Reeves WB. Effects of chloride channel blockers on hypoxic injury in rat proximal tubules. *Kidney Int*. 1997;51(5):1529–1534.
8. Waters SL, Scnellmann RG. Extracellular acidosis and chloride channel inhibitors act in the late phase of cellular injury to prevent death. *J Pharmacol Exp Ther*. 1996;278(3):1012–1017.
9. Venkatachalam MA, Weinberg JM, Patel Y, Saikumar P, Dong Z. Cytoprotection of kidney epithelial cells by compounds that target amino acid gated chloride channels. *Kidney Int*. 1996;49(2):449–460.
10. Burke TJ, Arnold PE, Gordon JA, Bulger RE, Dobyan DC, Schrier RW. Protective effect of intrarenal calcium membrane blockers before or after renal ischemia. Functional, morphological, and mitochondrial studies. *J Clin Invest*. 1984;74(5):1830–1841.
11. Pompermayer K, et al. The ATP-sensitive potassium channel blocker glibenclamide prevents renal ischemia//reperfusion injury in rats. *Kidney Int*. 2005;67(5):1785–1796.
12. Uchida K, et al. Lack of TRPM2 impaired insulin secretion and glucose metabolisms in mice. *Diabetes*. 2011;60(1):119–126.
13. Yamamoto S, et al. TRPM2-mediated Ca^{2+} influx induces chemokine production in monocytes that aggravates inflammatory neutrophil infiltration. *Nat Med*. 2008;14(7):738–747.
14. Hecquet CM, et al. Cooperative interaction of trp melastatin channel transient receptor potential (TRPM2) with its splice variant TRPM2 short variant is essential for endothelial cell apoptosis. *Circ Res*. 2014;114(3):469–479.
15. Zhang W, et al. A novel TRPM2 isoform inhibits calcium influx and susceptibility to cell death. *J Biol Chem*. 2003;278(18):16222–16229.
16. Zhang W, et al. TRPM2 is an ion channel that modulates hematopoietic cell death through activation of caspases and PARP cleavage. *Am J Physiol Cell Physiol*. 2006;290(4):C1146–C1159.
17. McNulty S, Fonfria E. The role of TRPM channels in cell death. *Pflugers Arch*. 2005;451(1):235–242.
18. Dietrich A, Chubanov V, Gudermann T. Renal TRPathies. *J Am Soc Nephrol*. 2010;21(5):736–744.
19. Qamar S, Vadivelu M, Sandford R. TRP channels and kidney disease: lessons from polycystic kidney disease. *Biochem Soc Trans*. 2007;35(pt 1):124–128.
20. Fonfria E, et al. Amyloid beta-peptide(1-42) and hydrogen peroxide-induced toxicity are mediated by TRPM2 in rat primary striatal cultures. *J Neurochem*. 2005;95(3):715–723.
21. Kolisek M, Beck A, Fleig A, Penner R. Cyclic ADP-ribose and hydrogen peroxide synergize with ADP-ribose in the activation of TRPM2 channels. *Mol Cell*. 2005;18(1):61–69.
22. Du J, Xie J, Yue L. Intracellular calcium activates TRPM2 and its alternative spliced isoforms. *Proc Natl Acad Sci U S A*. 2009;106(17):7239–7244.

23. Miller BA. The role of TRP channels in oxidative stress-induced cell death. *J Membr Biol*. 2006;209(1):31–41.
24. Cheung JY, Bonventre JV, Malis CD, Leaf A. Calcium and ischemic injury. *N Engl J Med*. 1986;314(26):1670–1676.
25. Donnahoo K, Meng X, Ayala A, Cain M, Harken A, Meldrum D. Early kidney TNF-a expression mediates neutrophil infiltration and injury after renal ischemia-reperfusion. *Am J Physiol*. 1999;277(3 pt 2):R922–R9R9.
26. Ueda N, Mayeux PR, Baliga R, Shah SV. Oxidant mechanisms in acute renal failure. In: Molitoris BA, Finn WF, eds. *Acute Renal Failure. A companion to Brenner & Rector's The Kidney.* Philadelphia, Pennsylvania, USA: WB Saunders Co.; 2001:60–77.
27. Heasman SJ, Ridley AJ. Mammalian Rho GTPases: new insights into their functions from in vivo studies. *Nat Rev Mol Cell Biol*. 2008;9(9):690–701.
28. Schulte BA, Spicer SS. Histochemical evaluation of mouse and rat kidneys with lectin-horseradish peroxidase conjugates. *Am J Anat*. 1983;168(3):345–362.
29. Reeves WB, Kwon O, Ramesh G. Netrin-1 and kidney injury. II. Netrin-1 is an early biomarker of acute kidney injury. *Am J Physiol Renal Physiol*. 2008;294(4):F731–F738.
30. Wang W, Reeves WB, Pays L, Mehlen P, Ramesh G. Netrin-1 overexpression protects kidney from ischemia reperfusion injury by suppressing apoptosis. *Am J Pathol*. 2009;175(3):1010–1018.
31. Mishra J, et al. Neutrophil gelatinase-associated lipocalin (NGAL) as a biomarker for acute renal injury after cardiac surgery. *Lancet*. 2005;365(9466):1231–1238.
32. Okusa M. The inflammatory cascade in acute ischemic renal failure. *Nephron*. 2002;90(2):133–138.
33. Togashi K, Inada H, Tominaga M. Inhibition of the transient receptor potential cation channel TRPM2 by 2-aminoethoxydiphenyl borate (2-APB). *Br J Pharmacol*. 2008;153(6):1324–1330.
34. Chen GL, Zeng B, Eastmond S, Elsenussi SE, Boa AN, Xu SZ. Pharmacological comparison of novel synthetic fenamate analogues with econazole and 2-APB on the inhibition of TRPM2 channels. *Br J Pharmacol*. 2012;167(6):1232–1243.
35. Wehrhahn J, Kraft R, Harteneck C, Hauschildt S. Transient receptor potential melastatin 2 is required for lipopolysaccharide-induced cytokine production in human monocytes. *J Immunol*. 2010;184(5):2386–2393.
36. Sumoza-Toledo A, et al. Dendritic cell maturation and chemotaxis is regulated by TRPM2-mediated lysosomal Ca^{2+} release. *FASEB J*. 2011;25(10):3529–3542.
37. Kaushal GP, Basnakian AG, Shah SV. Apoptotic pathways in ischemic acute renal failure. *Kidney Int*. 2004;66(2):500–506.
38. Paller MS, Hoidal JR, Ferris TF. Oxygen free radicals in ischemic acute renal failure in the rat. *J Clin Invest*. 1984;74(4):1156–1164.
39. Bedard K, Krause KH. The NOX family of ROS-generating NADPH oxidases: physiology and pathophysiology. *Physiol Rev*. 2007;87(1):245–313.
40. Bezzerides VJ, Ramsey IS, Kotecha S, Greka A, Clapham DE. Rapid vesicular translocation and insertion of TRP channels. *Nat Cell Biol*. 2004;6(8):709–720.
41. Raz L, et al. Role of Rac1 GTPase in NADPH oxidase activation and cognitive impairment following cerebral ischemia in the rat. *PLoS One*. 2010;5(9):e12606.
42. Gao Y, Dickerson JB, Guo F, Zheng J, Zheng Y. Rational design and characterization of a Rac GTPase-specific small molecule inhibitor. *Proc Nat Acad Sci USA*. 2004;101(20):7618–7623.
43. Miller BA, et al. The second member of transient receptor potential-melastatin channel family protects hearts from ischemia-reperfusion injury. *Am J Physiol Heart Circ Physiol*. 2013;304(7):H1010–H1022.
44. Hiroi T, et al. Neutrophil TRPM2 channels are implicated in the exacerbation of myocardial ischaemia/reperfusion injury. *Cardiovasc Res*. 2013;97(2):271–281.
45. Di A, et al. The redox-sensitive cation channel TRPM2 modulates phagocyte ROS production and inflammation. *Nat Immunol*. 2012;13(1):29–34.
46. Bonventre JV, Cheung JY. Effects of metabolic acidosis on viability of cells exposed to anoxia. *Am J Physiol*. 1985;249(1 pt 1):C149–C159.
47. Zager RA, Altschuld R. Body temperature: an important determinant of severity of ischemic renal injury. *Am J Physiol*. 1986;251(1 pt 2):F87–F93.
48. Filipovic DM, Reeves WB. Hydrogen peroxide activates glibenclamide sensitive K^+ channels in LLC-PK1 cells. *Am J Physiol*. 1997; 272(2 pt 1):C737–C743.
49. Lange I, Yamamoto S, Partida-Sanchez S, Mori Y, Fleig A, Penner R. TRPM2 functions as a lysosomal Ca^{2+}-release channel in β cells. *Sci Signal*. 2009;2(71):ra23.
50. Miller BA, et al. TRPM2 channels protect against cardiac ischemia-reperfusion injury: role of mitochondria. *J Biol Chem*. 2014;289(11):7615–7629.
51. Jia J, et al. Sex differences in neuroprotection provided by inhibition of TRPM2 channels following experimental stroke. *J Cereb Blood Flow Metab*. 2011;31(11):2160–2168.
52. Nicoud IB, et al. 2-APB protects against liver ischemia-reperfusion injury by reducing cellular and mitochondrial calcium uptake. *Am J Physiol Gastrointest Liver Physiol*. 2007;293(3):G623–G630.
53. Ohnuma Y, et al. Opening of mitochondrial KATP channel occurs downstream of PKC-epsilon activation in the mechanism of preconditioning. *Am J Physiol Heart Circ Physiol*. 2002;283(1):H440–H447.
54. Molitoris BA. Therapeutic translation in acute kidney injury: the epithelial/endothelial axis. *J Clin Invest*. 2014;124(6):2355–2363.
55. Hecquet CM, Ahmmed GU, Vogel SM, Malik AB. Role of TRPM2 channel in mediating H_2O_2-induced Ca^{2+} entry and endothelial hyperpermeability. *Circ Res*. 2008;102(3):347–355.
56. Sumoza-Toledo A, Penner R. TRPM2: a multifunctional ion channel for calcium signalling. *J Physiol*. 2011;589(pt 7):1515–1525.
57. Filipovic DM, Meng X, Reeves WB. Inhibition of poly(ADP-ribose)polymerase prevents oxidant-induced necrosis but not apoptosis in LLC-PK1 cells. *Am J Physiol*. 1999;277(3 pt 2):F428–F436.
58. Martin DR, Lewington AJP, Hammerman MR, Padanilam BJ. Inhibition of poly(ADP-ribose) polymerase attenuates ischemic renal injury in rats. *Am J Physiol Regul Integr Comp Physiol*. 2000;279(5):R1834–R1R40.
59. Zheng J, Devalaraja-Narashimha K, Singaravelu K, Padanilam BJ. Poly(ADP-ribose) polymerase-1 gene ablation protects mice from ischemic renal injury. *Am J Physiol Renal Physiol*. 2005;288(2):F387–FF98.
60. Basile DP, Liapis H, Hammerman MR. Expression of bcl-2 and bax in regenerating rat renal tubules following ischemic injury. *Am J Physiol*. 1997;272(5 pt 2):F640–F647.
61. Chien CT, Chang TC, Tsai CY, Shyue SK, Lai MK. Adenovirus-mediated bcl-2 gene transfer inhibits renal ischemia/reperfusion induced tubular oxidative stress and apoptosis. *Am J Transplant*. 2005;5(6):1194–1203.
62. Suzuki C, et al. Bcl-2 protects tubular epithelial cells from ischemia reperfusion injury by inhibiting apoptosis. *Cell Transplant*. 2008;17(1–2):223–229.
63. Orrenius S, Zhivotovsky B, Nicotera P. Regulation of cell death: the calcium-apoptosis link. *Nat Rev Mol Cell Biol*. 2003;4(7):552–565.
64. Kamata H, Honda S, Maeda S, Chang L, Hirata H, Karin M. Reactive oxygen species promote TNFα-induced death and sustained JNK activation by inhibiting MAP kinase phosphatases. *Cell*. 2005;120(5):649–661.
65. Yu H, et al. Rac1 activation in podocytes induces rapid foot process effacement and proteinuria. *Mol Cell Biol*. 2013;33(23):4755–4764.
66. Akilesh S, et al. Arhgap24 inactivates Rac1 in mouse podocytes, and a mutant form is associated with familial focal segmental glomerulosclerosis. *J Clin Invest*. 2011;121(10):4127–4137.
67. Blattner SM, et al. Divergent functions of the Rho GTPases Rac1 and Cdc42 in podocyte injury. *Kidney Int*. 2013;84(5):920–930.
68. Babelova A, et al. Activation of Rac-1 and RhoA contributes to podocyte injury in chronic kidney disease. *PLoS One*. 2013;8(11):e80328.
69. Lin L, Jin Y, Mars WM, Reeves WB, Hu K. Myeloid-derived tissue-type plasminogen activator promotes macrophage motility through FAK, Rac1, NF-κB pathways. *Am J Pathol*. 2014;184(10):2757–2767.
70. Ozaki M, et al. Inhibition of the Rac1 GTPase protects against nonlethal ischemia/reperfusion-induced necrosis and apoptosis in vivo. *FASEB J*. 2000;14(2):418–429.
71. Shan L, et al. Disruption of Rac1 signaling reduces ischemia–reperfusion injury in the diabetic heart by inhibiting calpain. *Free Radic Biol Med*. 2010;49(11):1804–1814.
72. Zhang QG, Wang R, Han D, Dong Y, Brann DW. Role of Rac1 GTPase in JNK signaling and delayed neuronal cell death following global cerebral ischemia. *Brain Res*. 2009;1265(Apr 10):138–147.
73. Sanlioglu S, et al. Lipopolysaccharide induces Rac1-dependent reactive oxygen species formation and coordinates tumor necrosis factor-α secretion through IKK regulation of NF-κB. *J Biol Chem*. 2001;276(32):30188–30198.
74. Altintas R, et al. The protective effects of apocynin on kidney damage caused by renal ischemia/reperfusion. *J Endourol*. 2013;27(5):617–624.
75. Tian D, et al. Antagonistic regulation of actin dynamics and cell motility by TRPC5 and TRPC6 channels. *Sci Signal*. 2010;3(145):ra77.

76. Schaldecker T, et al. Inhibition of the TRPC5 ion channel protects the kidney filter. *J Clin Invest*. 2013;123(12):5298–5309.
77. Zhang B, Ramesh G, Norbury C, Reeves WB. Cisplatin-induced nephrotoxicity is mediated by tumor necrosis factor-α produced by renal parenchymal cells. *Kidney Int*. 2007;72(1):37–44.
78. Ramesh G, Reeves WB. TNFR2-mediated apoptosis and necrosis in cisplatin-induced acute renal failure. *Am J Physiol Renal Physiol*. 2003;285(4):F610–F618.
79. Ramesh G, Reeves WB. TNF-α mediates chemokine and cytokine expression and renal injury in cisplatin nephrotoxicity. *J Clin Invest*. 2002;110(6):835–842.
80. Zhang B, Ramesh G, Uematsu S, Akira S, Reeves WB. TLR4 signaling mediates inflammation and tissue injury in nephrotoxicity. *J Am Soc Nephrol*. 2008;19(5):923–932.
81. Tadagavadi RK, Reeves WB. Renal dendritic cells ameliorate nephrotoxic acute kidney injury. *J Am Soc Nephrol*. 2010;21(1):53–63.
82. Tadagavadi RK, Reeves WB. Endogenous IL-10 attenuates cisplatin nephrotoxicity: role of dendritic cells. *J Immunol*. 2010;185(8):4904–4911.
83. Yu K, Qu Z, Cui Y, Hartzell HC. Chloride channel activity of bestrophin mutants associated with mild or late-onset macular degeneration. *Invest Ophthalmol Vis Sci*. 2007;48(10):4694–4705.
84. Terryn S, et al. A primary culture of mouse proximal tubular cells, established on collagen-coated membranes. *Am J Physiol Renal Physiol*. 2007;293(2):F476–F485.
85. Li Y, et al. Myocardial ischemia activates an injurious innate immune signaling via cardiac heat shock protein 60 and Toll-like receptor 4. *J Biol Chem*. 2011;286(36):31308–31319.
86. Ford BM, Eid AA, Gooz M, Barnes JL, Gorin YC, Abboud HE. ADAM17 mediates Nox4 expression and NADPH oxidase activity in the kidney cortex of OVE26 mice. *Am J Physiol Renal Physiol*. 2013;305(3):F323–F332.
87. Liu H, et al. Nitro-oleic acid protects the mouse kidney from ischemia and reperfusion injury. *Am J Physiol Renal Physiol*. 2008;295(4):F942–F949.